Integrated Fault Tolerant Scheme with Disturbance Feedforward

D.U. Campos-Delgado*
Fac. de Ciencias, UASLP
Av. Salvador Nava s/n
Zona Universitaria
C.P. 78290, S.L.P., Mexico
ducd@fc.uaslp.mx

S. Martínez Martínez
CIEP, Fac. de Ing., UASLP
Dr. Manuel Nava No.8
Zona Universitaria
C.P. 78290, S.L.P., Mexico
sinuhe@fc.uaslp.mx

K. Zhou
Dept. of Electrical and
Computer Engineering
Louisiana State University
Baton Rouge, LA 70803
kemin@ece.lsu.edu

***Abstract*— In this paper, an integrated fault-tolerant scheme is presented with disturbance compensation. Fault-detection and compensation are merged together to provide a robust algorithm against model uncertainties. The GIMC control architecture is used as a feedback configuration for the fault-tolerant scheme. The synthesis procedure for the parameters of the fault-tolerant scheme is carried out by using tools of robust control theory. In order to increase the set of strongly detectable faults, the disturbance information is feedforward into the fault detection algorithm. A detection filter is designed for fault isolation taking into account uncertainties in the mathematical model. Finally, the fault compensation strategy also incorporates the disturbance estimation to improve the performance of the closed-loop systems after the fault is detected. In order to illustrate these ideas, the speed regulation of a dc motor is selected as a case study, and experimental results are reported.**

I. Introduction

In many industrial applications, costly equipment is managed and human operators are involved. In this conditions, it is desirable to provide some safety degree into the process. Thus, the human operator must receive an indication of the possible faults into the process in order to take proper action: continue or stop it. If the fault is not severe, it is possible that the control system could be reconfigurated or compensated to maintain the closed-loop performance. Fault-tolerant control has emerged as a new necessity of the industry, pursuing to provide certain safety degree into the automated processes. For a fault-tolerant feedback configuration, the first challenge is fault detection. Consequently, a fault condition has to be detected by an algorithm capable of distinguishing among possible disturbances, noise and actual faults [3]. Thus, filters are designed such that the effect of faults is maximized at the outputs while the effect of disturbances is minimized. Besides fault detection, it is also important to isolate the faults. In this way, the operator can have some indication of location of the fault into the system. Several approaches have been suggested: robust detection and isolation based on eigenstructure assignment [10], estimation based on H_∞ optimization [4], detection and isolation by frequency domain optimization [9], detection based on model-based probabilistic approaches [5], etc. Furthermore, the applications of fuzzy logic [1] and wavelet transforms [13] to fault detection have been recently introduced.

One way of synthesizing fault-tolerant controllers is by appealing to H_∞ robust design techniques [3], [15]. However, these controllers tend to be very conservative in the practice. Recently, inspired by the Youla parmeterization used in robust control theory, a reconfigurable control structure for fault-tolerant control have been suggested in [2]. This scheme applies the GIMC (Generalized Internal Mode Control) structure introduced in [14] to design a control compensation signal after a fault is detected. On the other hand, reconfigurable fault tolerant structures have also been studied with different perspectives, as the model-matching strategy used in [7] and [12], and adaptive compensation [11].

The paper is structured as follows. Section 2 describes the problem formulation. The theory about the fault detection and compensation strategies are shown in Section 3. Section 4 gives a description of the case study: speed regulation of a dc motor. Finally, Section 5 gives some concluding remarks.

II. Problem Formulation

The problem addressed in this paper is formulated as follows. Consider an LTI system $P(s)$ affected by disturbances $d \in R^r$ and possible faults $f \in R^s$ (additive) described by

$$\begin{aligned} \dot{x} &= Ax + Bu + F_1 f + E_1 d \\ y &= Cx + Du + F_2 f + E_2 d \end{aligned} \tag{1}$$

where $x \in R^n$ represents the vector of state, $u \in R^m$ the vector of input, and $y \in R^p$ the the vector of output. Thus, the matrix $F_1 \in R^{n\times s}$ stands for the distribution matrix of the actuator faults and $F_2 \in R^{p\times s}$ for the sensor faults. Assume that a nominal controller $K(s)$ stabilizes the nominal plant $P(s)$ and it provides a desired closed-loop performance. Consequently, the **control objective** is presented as: *design an integrated fault-tolerant scheme such that it detects the occurrence of a fault in the closed-loop system, and provides an appropriate compensation signal q to the control system in order to maintain some closed-loop performance*. Two key assumptions are made in the problem formulation:

- The fault is non-repetitive.
- The disturbance is known or partially known.

The faults addressed in the paper assume that the control system suffers a severe deterioration in its dynamics after

*This research is supported in part by a grant from PROMEP, CONACYT, NASA and LEQSF

the fault is triggered, and consequently the process will have to stop in the case of no-compensation. Therefore, it is considered that the faults are non-repetitive. Now, in the reconfigurated control system, the performance after the fault is compensated will be largely dependant on the disturbance effect. In some cases, this information could be estimated from the measurements or directly measured (feedforward), in order to provide compensation. Thus, in this work, it is assumed that the possible disturbances in the feedback system are known or estimated.

The system response y can be analysed in the transfer matrix form:

$$Y(s) = P_{uy}(s)U(s) + P_{fy}(s)F(s) + P_{dy}(s)D(s) \quad (2)$$

where $P_{uy} = C(sI - A)^{-1}B + D$ (nominal plant), $P_{fy} = C(sI - A)^{-1}F_1 + F_2$, and $P_{dy} = C(sI - A)^{-1}E_1 + E_2$. Assume that there exists knowledge about the model uncertainties in the description of the nominal plant [15]. Two possible scenarios can be seen: unstructured or structured uncertainty.

- In the case that the uncertainty could be considered unstructured, the real plant $\hat{P}_{uy}$ is given by

$$\hat{P}_{uy}(s) = P_{uy}(s) + W_2(s)\Delta(s)W_1(s) \quad (3)$$

  where $W_1(s), W_2(s) \in RH_\infty$ are weighting functions for the uncertainty, and $\Delta \in RH_\infty$ with $\|\Delta\|_\infty < 1$.
- If the uncertainty can be derived from certain parameters of the model, where a range of variation can be deduced, then a structured uncertainty is adopted. As a consequence, the real plant can be represented by a lower linear fractional transformation (LFT):

$$\hat{P}_{uy}(s) = \mathcal{F}_l(\mathbf{P}, \Delta) = \mathbf{P}_{22} + \mathbf{P}_{21}\Delta(I - \mathbf{P}_{11}\Delta)^{-1}\mathbf{P}_{12} \quad (4)$$

  where

$$\mathbf{P} = \begin{bmatrix} \mathbf{P}_{11} & \mathbf{P}_{12} \\ \mathbf{P}_{21} & \mathbf{P}_{22} \end{bmatrix} \quad (5)$$

  $\Delta = diag[\delta_1 \delta_2 \dots \delta_k]$ with $\delta_i \in (-1, 1)$, and k represents the number of uncertain parameters. In this case, the generalized plant $\mathbf{P}$ is derived by pulling out the variation parameters δ_i from the nominal plant. Note that for the nominal plant $P_{uy} = \mathbf{P}_{22}$.

In this paper, the fault detection and compensation schemes are model-based. Therefore, assume that the nominal plant can be expressed by a left coprime factorization, i.e. $P_{uy} = \tilde{M}^{-1}\tilde{N}$ where $\tilde{N}, \tilde{M} \in RH_\infty$. Then a residual signal can be constructed by [3]:

$$R(s) = H(s)[-\tilde{N}(s)U(s) + \tilde{M}(s)Y(s)] \quad (6)$$

where $H \in RH_\infty$ is known as detection filter. By substituting (2) and assuming model uncertainty, it is obtained that

$$R(s) = H(s)[\tilde{M}(s)\Delta_{uy}(s)U(s) + \tilde{N}_d(s)D(s) + \tilde{N}_f(s)F(s)] \quad (7)$$

where $\Delta_{uy} = W_2(s)\Delta(s)W_1(s)$ for unstructured uncertainty and $\Delta_{uy} = \mathbf{P}_{21}\Delta(I - \mathbf{P}_{11}\Delta)^{-1}\mathbf{P}_{12}$ for structured, $P_{uf} = \tilde{M}^{-1}\tilde{N}_f$, and $P_{ud} = \tilde{M}^{-1}\tilde{N}_d$ with $\tilde{N}_d, \tilde{N}_f \in RH_\infty$. As a consequence, the residual signal is affected by the control signal, the perturbations and the faults. In order to detect a fault, the following residual evaluation criteria can be followed

$$\|r\| = \|r\|_{2,t,T} = \sqrt{\int_{t-T}^{t} r^*(\tau)r(\tau)d\tau} \quad (8)$$

$$\|r\| = \|r\|_\infty = \sup_t \|r\|_2 \quad (9)$$

where T is the window length or horizon of evaluation. Hence to avoid a false alarm in the evaluation due to perturbations or model uncertainties, a threshold value is selected

$$J_{th} = \sup_{f=0,d,u} \|r\| \quad (10)$$

Define the set of strongly detectable faults

$$\Upsilon = \{f | \inf_{d,u} \|r\| \geq J_{th}\} \quad (11)$$

Consequently, the filter $H(s)$ must be designed to maximize the size of Υ, i.e.

- $H(s)\tilde{M}(s)\Delta_{uy}(s) \approx 0$ and $H(s)\tilde{N}_d(s) \approx 0$,
- $H(s)\tilde{N}_f(s) \neq 0$ and as large as possible in some sense.

Note that if fault isolation is also pursued then $H(s)\tilde{N}_f(s) \approx I$.

III. Fault-Tolerant Scheme

In this section, the integrated fault-tolerant strategy is going to be described in detail.

A. Generalized Internal Model Control

The fault-tolerant architecture proposed in this work is derived from robust control theory [15], where a new implementation of the Youla parameterization called *Generalized Internal Mode Control (GIMC)* is used [2],[14]. In this configuration, the nominal controller K is represented by its left coprime factorization, i.e. $K = \tilde{V}^{-1}\tilde{U}$ such that $\tilde{U}, \tilde{V} \in RH_\infty$. This new control structure looks to overcome the classical conflict between performance and robustness in the traditional feedback framework.

A new implementation of the GIMC architecture is suggested in Figure 1. It is assumed that the disturbance d is known or partially known. Therefore, this information can be feedforward into the estimation process to cancel its effect from the filtered error f_e. Note that the residual signal proposed in the previous section, see (6), can be constructed by taking the signal f_e and process it through the detection filter $H(s)$, i.e. $R(s) = -H(s)F_e(s)$. Now, once the fault is detected, the compensation signal q is fed back into the controller structure, where q is also constructed from the filtered error f_e but through the robustification controller Q. Therefore, the signal q has to compensate the control signal by the missing/erroneous information due to the fault.

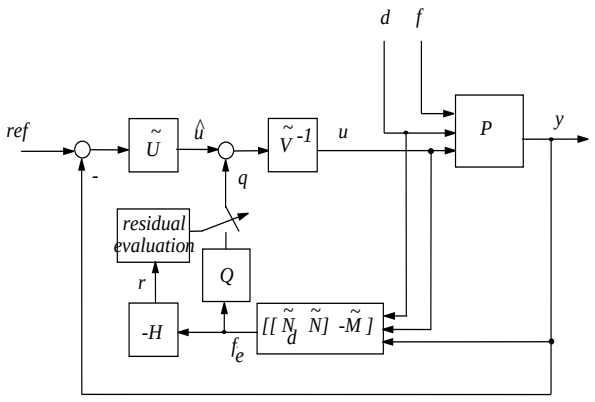

Fig. 1. Overall Fault-Tolerant Strategy.

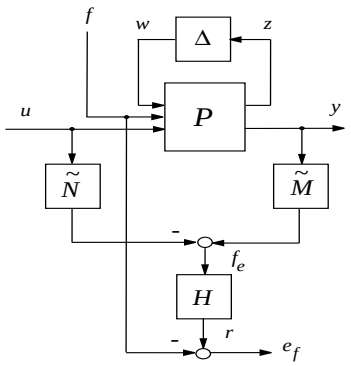

Fig. 2. Fault Detection Synthesis Diagram.

Consequently, a integrated fault-tolerant scheme can be achieved, as shown in Figure 1. As a result, the fault-tolerant scheme presents two free parameters to be designed:

1) $H(s)$: the fault detection filter that must diminish the effect of the disturbances or uncertainty into the residual signal, and maximize the effect of the faults.
2) $Q(s)$: the robustification controller that must provide robustness into the closed-loop system in order to maintain acceptable performance against faults.

The design strategies for these two parameters are presented next.

B. Fault Diagnosis

To design a robust detection filter $H(s)$, the information of the model uncertainties have to be incorporated. Since the information of the disturbances is feedforward into the estimation process, they are not consider during the design stage of the detection filter $H(s)$. However, the effect of disturbances could be also incorporated in the design framework. Assume that it is desired to isolate the faults, i.e. $r \approx f$, and define the estimation error for the faults $e_f = r - f$. Then, the performance objective of the filter can be stated as:

$$\min_{H \in RH_\infty} \|T_{e_f \nu}\|_\infty \quad \|\Delta\|_\infty < 1 \tag{12}$$

according to the synthesis diagram in Figure 2, where $\nu = [f\ u]^T$. Thus, the design problem can be tackled with tools from robust control theory: μ-synthesis [15].

C. Fault Compensation

In the design of the fault compensation signal q, the transfer matrix Q is chosen to maintain stability against faults. Only one limitation on this transfer matrix is considered, according with the Youla parameterization, it has to be stable, i.e. $Q \in RH_\infty$. *The synthesis process is again carried out through the philosophy of robust control*. In general, the sensor and actuator faults can be modeled in a multiplicative form $\tilde{y}(s) = [I + \Delta_s]y(s)$, and $\tilde{u}(s) = [I + \Delta_a]u(s)$ where $\Delta_s, \Delta_a \in RH_\infty$ represent the sensor and actuator perturbations due to the faults [2]. Consequently, if these terms are appended to the nominal plant P_{uy}, then the faulted input-output mapping $\tilde{P}_{uy}$ can be represented as

$$\begin{aligned} \tilde{P}_{uy} &= P_{uy}[I + \Delta_a] \quad \text{(actuator fault)} \\ \tilde{P}_{uy} &= [I + \Delta_s]P_{uy} \quad \text{(sensor fault)} \end{aligned} \tag{13}$$

Thus the sensor or actuator faults can be modeled as output or input model uncertainties respectively. As mentioned before, we shall consider a basic robustness requirement in this paper, i.e. the closed-loop stability. Hence our objective is to design Q to maximize the failure tolerance in the closed-loop system, i.e.

$$\min_{Q} \|T_{zw}\|_\infty \tag{14}$$

where T_{zw} is the closed-loop transfer function from signals w to z. Two design scenarios can be presented according with the stability of the nominal plant $P_{uy}(s)$ [2]:

1) $P_{uy} \in RH_\infty \quad \Rightarrow$ the optimal compensator is given by $Q = -\tilde{U}\tilde{M}^{-1}$, for any plant and type of uncertainty description.
2) $P_{uy} \notin RH_\infty \quad \Rightarrow$ a weighted H_∞ approximation has to be solved. For this purpose, the synthesis problem can be put into an LFT framework, as seen in Figure 3. Hence, Q is chosen according to

$$\gamma = \min_{Q} \|\mathcal{F}_l(\mathbf{G}, Q)\|_\infty \tag{15}$$

and internal stability is guaranteed if $\|\Delta\|_\infty < 1/\gamma$. If an output uncertainty (sensor fault) is considered (i.e. $\tilde{P}_{uy} = [I + \Delta_s]P_{uy}$), the generalized plant $\mathbf{G}$ will be given by

$$\mathbf{G} = \begin{bmatrix} -\tilde{S}P_{uy}K & \tilde{S}P_{uy}\tilde{V}^{-1} \\ -\tilde{M} & 0 \end{bmatrix} \tag{16}$$

where $\tilde{S} = (I + P_{uy}K)^{-1}$. Note that in this case $\gamma \geq 1$ since this will represent that the maximum tolerable uncertainty is always $\|\Delta_s\|_\infty < 1$. Otherwise, the uncertainty could take the value $\Delta_s = -I$ (sensors outage) and the closed-loop will become unstable.

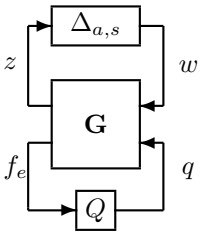

Fig. 3. Generalized linear fractional transformation.

Remark 1: It is important to mention that if there is some delay in the detection of the fault triggering, this will affect the performance of the reconfigurated control system. Furthermore, it is possible that the system could not be stabilized if there is a significant delay in the detection process. As it was seen experimentally, this delay is a factor of the speed of response of the nominal controller. Hence, if the controller has fast dynamics, the tolerable delay is reduced.

IV. Case Study: Speed Regulation of a DC Motor

To illustrate the mentioned fault-tolerant technique, the application to a dc-motor speed drive is presented next [8]. The test-bed setup is shown in Figure 4, and it consists of a 1 HP dc-motor connected to a 3/4 HP permanent magnet dc-motor. The later one acts as a generator in order to provide a load to the shunt dc-motor. In this setup, the load torque varies according with the angular frequency. The fault-tolerant algorithm was implemented in a dSpace DS1103 system under the environment of MATLAB/Simulink ©. The algorithms were run under a sampling frequency of $10kHz$. In the implementation, there are measurements of electrical currents made by Hall-effect sensors, and angular velocity by a tacogenerator of $50V/1000$ RPM and $\pm 5\%$ tolerance.

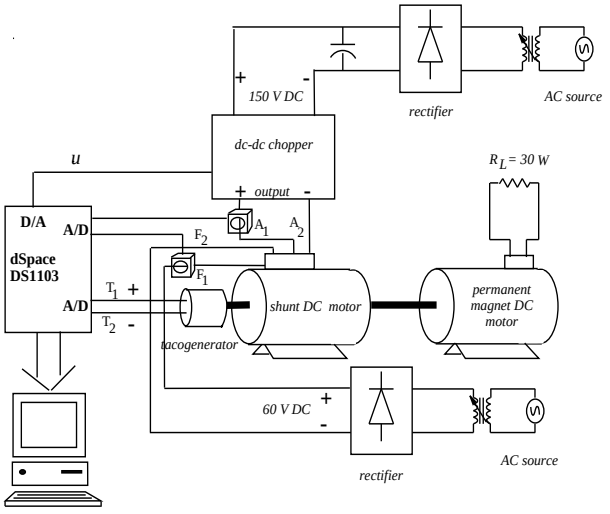

Fig. 4. Test-bed Setup.

TABLE I
DC Motor Parameters.

$R_a = 3.72\,\Omega$	Armature Resistance
$L_a = 7.83\,mH$	Armature Inductance
$B = 2.59 \times 10^{-4}\,N\,m/rad/s$	Friction Coefficient
$J = 2.72 \times 10^{-3}\,kg\,m$	Inertia
$K_b = 0.31\,V/rad/s$	Electromagnetic Constant
$R_f = 87.3\,\Omega$	Field Resistance
$L_f = 9.22\,H$	Field Inductance
$\omega_0 = 1500\,rpm$	Nominal Velocity
$V_r = 90\,V$	Rated Armature Voltage
$I_{max} = 10\,A$	Maximum Armature Current

A. Model Description

The dc-motor is considered in the separated excitation configuration. Thus, the field voltage v_f is fixed to a constant value and the armature voltage v_a is varied in order to regulate the angular velocity ω of the motor. Two measurements are available for feedback purposes: armature current i_a and angular velocity ω. Thus, the dc-motor is modelled as a system with one-input (v_a) and two-outputs (i_a and ω):

$$\begin{bmatrix} \dot{i_a} \\ \dot{\omega} \end{bmatrix} = \begin{bmatrix} \frac{-R_a}{L_a} & -\frac{K_b}{L_a} \\ \frac{K_b}{J} & -\frac{B}{J} \end{bmatrix} \begin{bmatrix} i_a \\ \omega \end{bmatrix} + \begin{bmatrix} \frac{1}{L_a} \\ 0 \end{bmatrix} v_a + \begin{bmatrix} 0 \\ -\frac{1}{J} \end{bmatrix} T_l \tag{17}$$

where the parameters of the dc-motor were obtained through a systematic experimental process [8], and they are shown in Table I. In the motor description, the load torque T_l is represented as a disturbance to the system, but this variable cannot be measured on real-time in the experimental system. Nevertheless, during the experiments, it is assumed to behave as a constant or present a very slow variation. In this way, its steady state value can be calculated from the angular velocity and armature current measurements:

$$\overline{T}_l = K_b i_a - B\omega \tag{18}$$

The armature voltage v_a is controlled by dc-dc chopper working under a PWM scheme (switching frequency $50kHz$), where the control parameter is the duty cycle. The chopper was selected as control actuator due to its fast response and linear dynamics. The construction of the actuator was carried out in our lab, and it is designed such that it is controlled by a voltage signal u in the interval $[0, 5V]$. This saturation in the control signal u did not limited the performance of the system. The control actuator (dc-dc chopper) was modeled as a first order system:

$$G_a(s) = \frac{V_a(s)}{U(s)} = K_a \frac{s+a}{s+b} \tag{19}$$

where the parameters of the model (K_a, a, b) were obtained experimentally by applying the theory of algebraic identification [6]. In the test setup, the control input to the actuator u was specified by a square wave and the angular velocity ω and armature current i_a were recorded without load considered. Note that it is not possible to record the armature voltage signal v_a, since the chopper is working at a fixed switching frequency of $50kHz$ and the data

TABLE II
CONTROL ACTUATOR PARAMETERS.

$K_a = 20.71$	Actuator Gain
$a = -6.66$	zero location
$b = 5.43$	pole location

acquisition is sampling at $10kHz$. Therefore, the armature voltage cannot be incorporated into the identification process. Thus, one input and two output signals of the systems are available to identify three parameters for the actuator. Six different experiments were carried out and the average value of the parameters K_a, a and b are given in Table II. In the overall, there exists some uncertainty in the description of some of the parameters including motor and actuator. Thus, for R_a, L_a, J, K_a, a and b, they can be associated with a parametric uncertainty description. As a consequence, a structured uncertainty description can be arranged for the open-loop system. This uncertainty description will be used to design the fault detection filter $H(s)$.

B. Design of Fault Tolerant Scheme

Note that with the parameters given to the nominal plant (17) and actuator (19), the open-loop system is stable. Next, the nominal controller K is designed to guarantee good step tracking capabilities. For this purpose, an LQG controller [15] is synthesized where integral action is appended to the controller since the original plant does not have any mode at the origin. This will improve the tracking capabilities of the closed-loop.

Using a structured uncertainty description for the plant, the optimization problem formulated in (12) was carried out to design $H(s)$. Thus, according with the diagram of Figure 2, the LFT is constructed to formulate the robust performance filter problem using μ-synthesis. The $D-K$ iteration was run and the resulting filter of order 21^{th} was reduced through balance truncation to 9^{th}. Finally, since the nominal plant and actuator dynamics are stable, then the compensation controller is selected $Q = -\tilde{U}\tilde{M}^{-1}$.

Once the residual signal (6) was constructed, the fault was detected according to the criterion:

$$\sup_t \|r\|_2 \geq J_{th} \tag{20}$$

where the threshold for detection is calculated by using the size of the uncertainty and the maximum value of the control signal

$$J_{th} = \|H(s)\tilde{M}(s)\Delta_{uy}(s)\|_1 \|u\|_\infty \tag{21}$$

C. Experimental Implementation

Next, the integrated fault-tolerant structure shown in Figure 1 was implemented first in simulation by using MATLAB/Simulink ©, and experimentally in the dSpace 1103 system. The disturbance estimation $\overline{T}_l$ in (18) was used to feedforward this information into the fault-tolerant control. Two abrupt faults were considered for the sensors:

1) **Case 1**: the angular velocity sensor ω is completely disconnected (tacogenerator) from the system at a given time,
2) **Case 2**: there is an outage of the armature current i_a sensor.

The failure cases were simulated by software in the dSpace system and not directly in the hardware. In both scenarios, the fault-tolerant system was able to compensate properly the control signal for these faults. The angular velocity reference for both cases was set to 1500 RPM. The experimental results for the tacogenerator fault are shown in Figure 5. Note that for the angular velocity fault, *the uncompensated closed-loop system becomes unstable with just one feedback measurement*. Thus, it is observed that the nominal control signal $\hat{u}$ starts to increase after the fault, since the controller assumes that the angular velocity has dropped suddenly its value to zero. However, the compensation signal q is capable of cancelling this effect, and the actual control signal u just decrease its value after the fault is active. It is noticeable that the reference is not maintained, this is due to the estimation of the torque T_l (disturbance) which is an approximation of the real value. As a consequence, the error in the estimation of the load torque affects the tracking capabilities of the overall system. Therefore, if this signal could be acquired by a direct measurement then the compensation will be more accurate. This behavior was seen during simulation. Now, in Figure 6, the experimental testing for a change of reference after a fault scenario (Case 1) is illustrated. This plot shows that the system still is able to follow a reference signal after the fault, but with a certain error.

Remark 2: During the experimental testing, other types of faults were investigated. Thus, a fault such that the sensor reduced its gain by certain percentage was investigated. In this case, the fault-tolerant scheme can successfully detect and compensate that fault. Besides abrupt faults, an incipient type of fault was also tested. Thus, the sensor measurement was slowly decaying after the triggering time. For this type fault, the main issue is fault detection, since according to the decaying rate of the measurement, the residual will take more or less time to overcome the detection threshold. However, the fault-tolerant algorithm can also compensate this fault, but there is some deterioration of the performance due to the delay time in the detection process. The implementation for this fault was only carried out in simulation, since there was a risk of damaging the dc-motor in the actual test-bed setup. Consequently, other detection algorithms could be applied to improve the size of the set of strongly detectable faults Υ, for example based on wavelet analysis and fuzzy logic .

V. CONCLUSIONS

An integrated fault-tolerant scheme was introduced. The strategy relies on information of the process and possible uncertainties. The GIMC control architecture is used as a feedback configuration for the fault-tolerant scheme. The

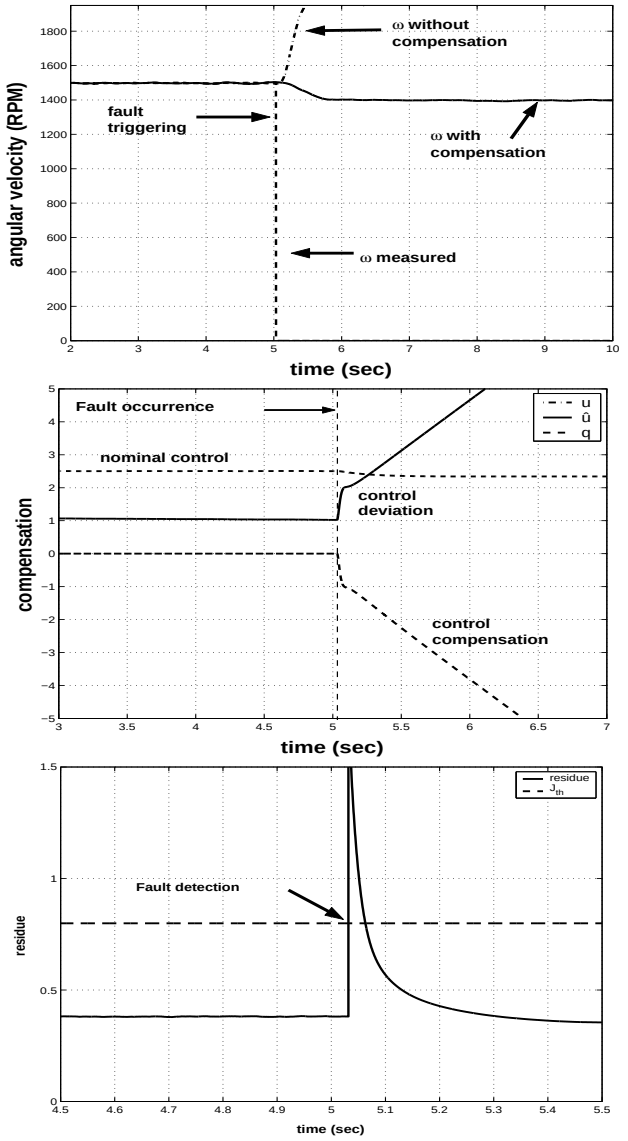

Fig. 5. Experimental Response with Angular Velocity ω Fault.

synthesis procedures were obtained by using robust control theory. The disturbances entering the system affect the performance of the compensated control system. Thus, this information is also fed back into the fault-tolerant architecture to cancel their effect. The speed regulation of a dc motor was selected as a case of study and the experimental results show the effectiveness of the proposed scheme.

REFERENCES

[1] S. Altug, M.Y. Chow, H.J. Trussell, "Fuzzy Inference Systems Implemented on Neural Architectures for Motor Fault Detection and Diagnosis," *IEEE Transactions on Industrial Electronics*, Vol. 46, No. 6, pp. 1063-1079, 1999.

[2] D.U. Campos-Delgado and K. Zhou, "Reconfigurable Fault Tolerant Control Using GIMC Structure", *IEEE Transactions on Automatic Control*, Vol. 48, No. 5, pp. 832-838, 2003.

[3] J. Chen and R.J. Patton, *Robust Model-Based Fault Diagnosis for Dynamic Systems*, Kluwer Academic Publishers, 1999.

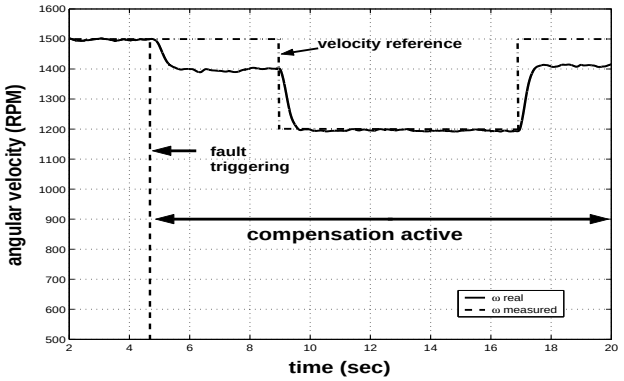

Fig. 6. Experimental Response with Angular Velocity Fault and Change of Reference.

[4] E.G. Collins Jr. and T. Song, "Robust H_∞ Estimation and Fault Detection of Uncertain Dynamic Systems," *Journal of Guidance, Control and Dynamics*, Vol. 23, No. 5, pp. 857-864, 2000.

[5] L. Dinca, T. Aldemir and G. Rizzoni, "A Model-Based Probabilistic Approach for Fault Detection and Identification with Application to the Diagnosis of Automotive Engines," *IEEE Transactions on Automatic Control*, Vol. 44, No. 11, pp. 2200-2205, 1999.

[6] M. Fliess and H. Sira-Ramírez, "An Algebraic Framework for Linear Identification", *ESAIM, Control, Optimization and Calculus of Variations*, Vol. 9, pp. 151-168, 2003.

[7] D. Kim and Y. Kim, "Robust Variable Structure Controller Design for Fault Tolerant Flight Control," *Journal of Guidance, Control and Dynamics*, Vol. 23, No. 3, pp. 430-437, 2000.

[8] R. Krishnan, *Electric Motor Drives: Modeling, Analysis, and Control*. Prentice-Hall, 2001.

[9] D. Sauter and F. Hamelin,"Frequency-Domain Optimization for Robust Fault Detection and Isolation in Dynamic Systems," *IEEE Transactions on Automatic Control*, Vol. 44, No. 4, pp. 878-882, 1999.

[10] L.C. Shen, S.K. Chang and P.L. Hsu, "Robust Fault Detection and Isolation with Unstructured Uncertainty Using Eigenstructure Assignment," *Journal of Guidance, Control and Dynamics*, Vol. 21, No. 1, pp. 50-57, 1998.

[11] G. Tao, S. Chen and S.M. Joshi, "An Adaptive Actuator Failure Compensation Controller Using Output Feedback," *IEEE Transactions on Automatic Control*, Vol. 47, No. 3, pp.506-511, 2002.

[12] Z. Yang and J. Stoustrup, "Robust Reconfigurable Control for Parametric and Additive Faults with FDI Uncertainties," in *Proc. IEEE Conf. Decision Control*, Sydney, Australia, 2000.

[13] H. Ye, S.X. Ding and G. Wang, "Integrated Design for Fault detection Systems in Time-Frequency Domain," *IEEE Transactions on Automatic Control* , Vol. 47, No. 2, pp. 384-390, 2002.

[14] K. Zhou and Z. Ren, "A New Controller Architecture for High Performance, Robust and Fault Tolerant Control," *IEEE Transactions on Automatic Control*, Vol. 46, No.10, pp. 1613-1618, 2001.

[15] K. Zhou, J.C. Doyle and K. Glover, *Robust and Optimal Control*. Prentice Hall, New Jersey, 1996.